Study on Flame Propagation Characteristics of Natural Gas–Hydrogen–Air Mixtures

ARTICLE *in* ENERGY & FUELS · OCTOBER 2006

Impact Factor: 2.79 · DOI: 10.1021/ef060334v

Zuohua Huang

Xi'an Jiaotong University

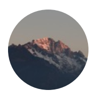

Yong Zhang

China Meteorological Administration

Haiyan Miao

Agency for Science, Technology and Researc…

Study on Flame Propagation Characteristics of Natural Gas–Hydrogen–Air Mixtures

Zuohua Huang,* Yong Zhang, Qian Wang, Jinhua Wang, Deming Jiang, and Haiyan Miao

State Key Laboratory of Multiphase Flow in Power Engineering, Xi'an Jiaotong University, Xi'an 710049, People's Republic of China

Received July 20, 2006. Revised Manuscript Received September 8, 2006

Flame propagation characteristics of natural gas–hydrogen–air mixtures were studied in a constant volume combustion bomb at room temperature and low initial pressures. The laminar burning velocities, the mass burning fluxes, and the Markstein number were obtained at various hydrogen fractions and equivalence ratios. The results show that the unstretched laminar burning velocity and the mass burning flux increase with the increase of hydrogen fraction in a natural gas–hydrogen blend. Flame stability tends to increase with the increase of equivalence ratio. For a specific equivalence ratio, the Markstein number decreases with the increase of hydrogen fraction, leading to an increase of thermodiffusively generated flame instability. Flaw and protruding or even honeycomb-like structure occur at the flame front area under lean mixture combustion while rich mixture combustion maintains a smooth flame front surface. Lean mixture increases flame instability while rich mixture increases flame stability. At a large hydrogen fraction (larger than 80%), ρ_u/ρ_b is increased and flame thickness is decreased with the increase of hydrogen fraction, leading to the increase of flame instability, and easily forms a cellular surface at flame front.

Introduction

With increasing concern about the energy shortage and environmental protection, research on improving engine fuel economy and reduction of the exhaust emissions have become a major research aspect in combustion community and engine development. Due to limited crude oil reserves, the development of the alternative fuel engines has attracted more and more interest in the engine community. Alternative fuels usually belong to the clean fuels as compared to the diesel fuel and gasoline fuel in engine combustion processes, thus the introduction of these alternative fuels is beneficial for slowing-down the fuel shortage and reduction of engine exhaust emissions. Natural gas is considered to be one of the favorable fuels for engines, and the natural gas fueled engine has been utilized in both the spark-ignited engine and the compression-ignited engine. However, due to the slow burning velocity of natural gas and the poor lean-burn capability, the natural gas spark-ignited engine has the disadvantage of low thermal efficiency, large cycle-by-cycle variations, and poor lean-burn ability. These will decrease the engine power output and increase fuel consumption.[1,2] Due to these restrictions, a natural gas engine is usually operated at the condition of stoichiometric equivalence ratio with relative low thermal efficiency. Traditionally, in order to improve the lean-burn capability and flame burning velocity of the natural gas engine under lean-burn condition, an increasing flow intensity in the cylinder is introduced. This measure always increases the heat loss to the cylinder wall and increases the combustion temperature as well as the NO_x emission.[3] One of the effective methods to solve the problem of slow burning velocity of natural gas is to mix the natural gas with a fuel that possesses a fast burning velocity. Hydrogen is regarded as the best gaseous candidate for natural gas due to its very fast burning velocity. This combination is expected to improve the lean-burn characteristics and decrease the engine emissions.[4,5]

Up to now, most work on burning velocities concentrates on pure methane[6] and pure hydrogen.[7] Some work has touched on methane–hydrogen–air flames.[8] Law et al. investigated the instability of expending hydrogen–propane spherical flames.[9] However, few reports on the flame stability of methane, natural gas–hydrogen, or methane–hydrogen flames were analyzed. Liao et al. measured the laminar burning velocity of natural gas based on the spherical flame pattern and found that the laminar burning velocity of natural gas was much closer to that of methane.[10] Yu et al. investigated the burning velocity of a

* Corresponding author. E-mail: zhhuang@mail.xjtu.edu.cn.

(1) Rousseau, S.; Lemoult, B.; Tazerout, M. Combustion characteristics of natural gas in a lean burn spark-ignition engine. *Proc. Inst. Mech. Eng., Part D, J. Automob. Eng.* **1999**, *213* (D5), 481–489.

(2) Ben, L.; Dacros, N. R.; Truquet, R.; Charnay, G. Influence of air/fuel ratio on cyclic variation and exhaust emission in natural gas SI engine. *SAE Tech. Pap.* **1999**, *No. 992901*.

(3) Das, A.; Watson, H. C. Development of a natural gas spark ignition engine for optimum performance. *Proc. Inst. Mech. Eng., Part D, J. Automob. Eng.* **1997**, *211* (D5), 361–378.

(4) Blarigan, P. V.; Keller, J. O. A Hydrogen fuelled internal combustion engine designed for single speed/power operation. *Int. J. Hydrogen Energy* **2002**, *23* (7), 603–609.

(5) Akansu, S. O.; Dulger, A.; Kahraman, N. Internal combustion engines fueled by natural gas–hydrogen mixtures. *Int. J. Hydrogen Energy* **2004**, *29* (14), 1527–1539.

(6) Gu, X. J.; Haq, M. Z.; Lawes, M. Laminar burning velocity and Markstein lengths of methane–air mixtures. *Combust. Flame* **2000**, *121* (1–2), 41–58.

(7) Lamoureux, N.; Djebaili-Chaumeix, N.; Paillard, C. E. Laminar flame velocity determination for H_2–air–He–CO_2 mixtures using the spherical bomb method. *Exp. Therm. Fluid Sci.* **2003**, *27* (4), 385–393.

(8) Halter, F.; Chauveau, C.; Djebayli-Chaumeix, N. Characterization of effects of pressure and hydrogen concentration on laminar burning velocities of methane–hydrogen–air mixture. *Proc. Combust. Inst.* **2005**, *30*, 201–208.

(9) Law, C. K.; Jomaas, G.; Bechtold, J. K. Cellular instabilities of expending hydrogen–propane spherical flames at elevated pressures: theory and experiment. *Proc. Combust. Inst.* **2005**, *30* (1), 159–167.

10.1021/ef060334v CCC: $33.50
Published on Web 10/19/2006

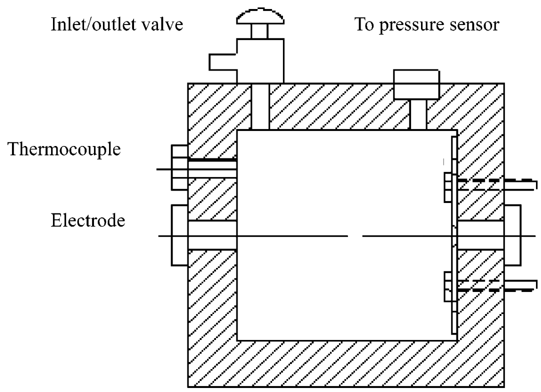

Figure 1. Constant volume combustion bomb.

Table 1. Compositions of Natural Gas

items	CH_4	C_2H_6	C_3H_8	N_2	CO_2	others
volumetric fraction (%)	96.160	1.096	0.136	0.001	2.540	0.067

methane-hydrogen mixture,[11] and Law and Kwon studied the flame propagation phenomenon of a mixture with 85% hydrogen and 15% methane.[12] Their studies showed that mixing of hydrogen into natural gas could remarkably increase the burning velocity of the mixture, but the flame instability would increase at a high hydrogen ratio. Previous research revealed the effectiveness of the natural gas−hydrogen combination for increasing the burning velocity. However, these previous works only supplied the information on the selected hydrogen fraction and at the stoichiometric equivalence ratio. There are still many fundamental aspects that need to be investigated, especially over the wide range of equivalence ratios and the wide range of hydrogen fractions. This quantitative information will be helpful in clarifying the flame propagation characteristics for the natural gas−hydrogen−air mixture combustion.

The objective of this paper was to investigate the flame characteristics of natural gas−hydrogen mixtures at various hydrogen fractions and various equivalence ratios by using the constant volume combustion bomb and to analyze flame stability based on the Markstein number and flame photos.

Experimental Procedures

The experiment was conducted in a constant volume combustion bomb as shown in Figure 1, and a detailed description of the experimental setup is in ref 10. The combustion bomb is a cuboid type with inside diameter of 108 × 108 × 135 mm. Two sides of this bomb are transparent to make the inside observable, which are to provide the optical access. The combustible mixture is prepared within the chamber by adding natural gas, hydrogen, and air at the specified partial pressures. The mixture is ignited by centrally located electrodes, and a standard capacitive discharge ignition system is used for producing the spark. In this study, the ignition energy is 45 mJ. The pressure is recorded by a piezoelectric Kistler absolute pressure transducer with a resolution of 0.01 kPa.

Hydrogen with purity of 99.995% is used, while natural gas constitution is listed in Table 1. Considering the formula of natural gas as $C_\alpha H_\beta O_\gamma$, it can be calculated that α is 1.01523, β is 3.928084, and γ is 0.05086. The combustible mixture in bomb can be expressed as $xC_\alpha H_\beta O_\gamma + (1 - x)H_2 + L(O_2 + 3.762N_2)$, and the equivalence ratio of the natural gas−hydrogen−air mixture is defined as $\phi = ((\alpha + \beta/4 - \gamma + 1/2)x + 1/2)/L$.

In the experiment, the initial pressure and temperature keep the same value for mixtures with different hydrogen fractions. The initial condition was strictly controlled in the experiments to realize the same initial pressure and temperature. For avoiding the influence of wall temperature on mixture temperature, a large enough interval between the two experiments is set, providing enough time for the wall to cool down and keeping the same initial temperature. As flame exhibits a spherical pattern, the flame radius was scaled from the flame photo recorded by a high-speed camera.

Laminar Burning Velocity and Markstein Length

The laminar burning velocity and Markstein number can be deduced from Schlieren photographs as described by Bradley et al.[13] For a spherically expanding flame, the stretched flame velocity (S_n), reflecting the flame propagation speed, is derived from the flame radius versus time data as

$$S_n = \frac{dr_u}{dt} \tag{1}$$

where r_u is the radius of flame in Schlieren photographs and t is the time. S_n can be directly obtained from the flame photo.

The Schlieren method detects the flame front by density gradient along the flame front due to a big difference in densities between the unburned gas and the burned gas. If the flame thickness is small, then the Schlieren photo can accurately detect the flame front; otherwise, there will be some error in detecting the flame front. For premixed mixture flame propagation, the flame front is smooth and flame thickness is small; thus, the Schlieren photos can accurately calculate the flame radius. In the case of large hydrogen fraction and/or lean mixture combustion, the flame front may develop into the cellular type in the late stage of flame propagation, and the determination of flame radius will be influenced by the cellular flame front. However, as shown in the photos, the scale of the cellular structure at flame front is much smaller than that of flame size; thus, the estimation of flame radius through Schlieren photograph is still highly accurate in determination of flame front. Thus, for premixed mixture expanding spherical flame, the flame radius can be calculated from the Schlieren photographs.

Flame stretch rate, α, representing the expanding rate of flame front area. in a quiescent mixture is defined as

$$\alpha = \frac{d(\ln A)}{dt} = \frac{1}{A}\frac{dA}{dt} \tag{2}$$

where A is the area of flame. For a spherically outwardly expanding flame front, the flame stretch rate can be simplified as

$$\alpha = \frac{1}{A}\frac{dA}{dt} = \frac{2}{r_u}\frac{dr_u}{dt} = \frac{2}{r_u}S_n \tag{3}$$

In respect to the early stage of flame expansion, there exists a linear relationship between the flame speeds and the flame stretch rates,[6] which is

$$S_l - S_n = L_b\alpha \tag{4}$$

(10) Liao, S. Y.; Jiang, D. M.; Gao, J. Measurements of Markstein numbers and laminar burning velocities for liquefied petroleum gas−air mixtures. *Fuel* **2004**, *83* (10), 1281−1288.

(11) Yu, G.; Law, C. K.; Wu, C. K. Laminar flame speeds of hydrogen + air mixtures with hydrogen addition. *Combust. Flame* **1986**, *63* (3), 339−347.

(12) Law, C. K.; Kwon, O. C. Effects of hydrocarbon substitution on atmospheric hydrogen−air flame propagation. *Int. J. Hydrogen Energy* **2004**, *29* (8), 867−879.

(13) Bradley, D.; Gaskell, P. H.; Gu, X. J. Burning velocities, Markstein lengths, and flame quenching for spherical methane−air flames: a computational study. *Combust. Flame* **1996**, *104* (1−2), 176−198.

where S_l is the unstretched flame speed, and L_b is the Markstein length (Markstein number) of burned gases.

For the premixed laminar flame, most previous works identify the flame front stability and/or instability through the flame front structure and variation during the flame propagation. If the flame front maintains a smooth front during flame propagation, then the flame is regarded as a stability flame. If the flame front cannot maintain a smooth front and or becomes a cellular type during flame propagation, then the flame is regarded as an instability flame

The burned gas Markstein number L_b is the slope of $S_n-\alpha$ curve. The Markstein number can reflect the stability of flame. A positive value of L_b indicates that the flame speed decreases with the increase of flame stretch rate if any kind of protuberances appear at flame front (stretch increasing), the flame speed at the flame protruding position will be suppressed, and this makes the flame stable. In contrast to this, a negative value of L_b means that the flame speed increases with the increase of flame stretch rate if any kind of protuberances appear at flame front, the flame speed at the flame protruding position will be increased, and this will increase the instability of the flame.[13] When the observation is limited to the initial part of the flame expansion, where the pressure does not vary significantly yet, then a simple relationship linking the spatial flame velocity (S_l) to the unstretched laminar burning velocity (U_l) is given by Law et al.[12] as

$$U_l = \rho_b S_l / \rho_u \tag{5}$$

Mass burning flux (f) is also given by Law et al.[12] as

$$f = \rho_b S_l \tag{6}$$

where ρ_b and ρ_u are the densities for burned gases and unburned gases, respectively. ρ_u uses the value of initial state, and ρ_b is determined from thermal equilibrium.

Results and Discussions

Laminar Burning Velocity. Figure 2 give the unstretched laminar burning velocity and the mass burning flux versus hydrogen fraction at three equivalence ratios. The results show that both unstretched laminar burning velocity and mass burning flux increase with the increase of hydrogen fraction, and their increasing rates gives a high value at a high hydrogen fraction. As the density of hydrogen is much less than that of natural gas, this will decrease the density of mixture, making the mass burning flux slightly less than unstretched laminar burning velocity. For lean mixture combustion and stoichiometric mixture combustion, the increment of mass burning flux is low and keeps almost the same value while the value is high at rich mixture combustion. For example, in the case of 80% fraction of hydrogen, the increments of mass burning fluxes to pure natural gas combustion at equivalence ratios of 0.7, 1.0, and 1.3 give the values of 2.89, 2.82, and 5.10, respectively.

Flame Stability. The instability of premixed flame is influenced by both thermodiffusive factor and hydrodynamic factor.[6,12] At the initial stage of flame development, the thermodiffusive factor plays a dominant role, and with the development of flame, the hydrodynamic factor becomes the larger influence factor. At the initial stage of flame propagation, the Markstein number can be used to reflect the sensitivity of flame stretched and the stability of flame. As shown in Figure 3, the Markstein number decreases with the increase of hydrogen fraction in natural gas−hydrogen blend. This indicates that the addition of hydrogen in natural gas will increase the instability of flame, and the instability of flame will increase the increase of hydrogen fraction.

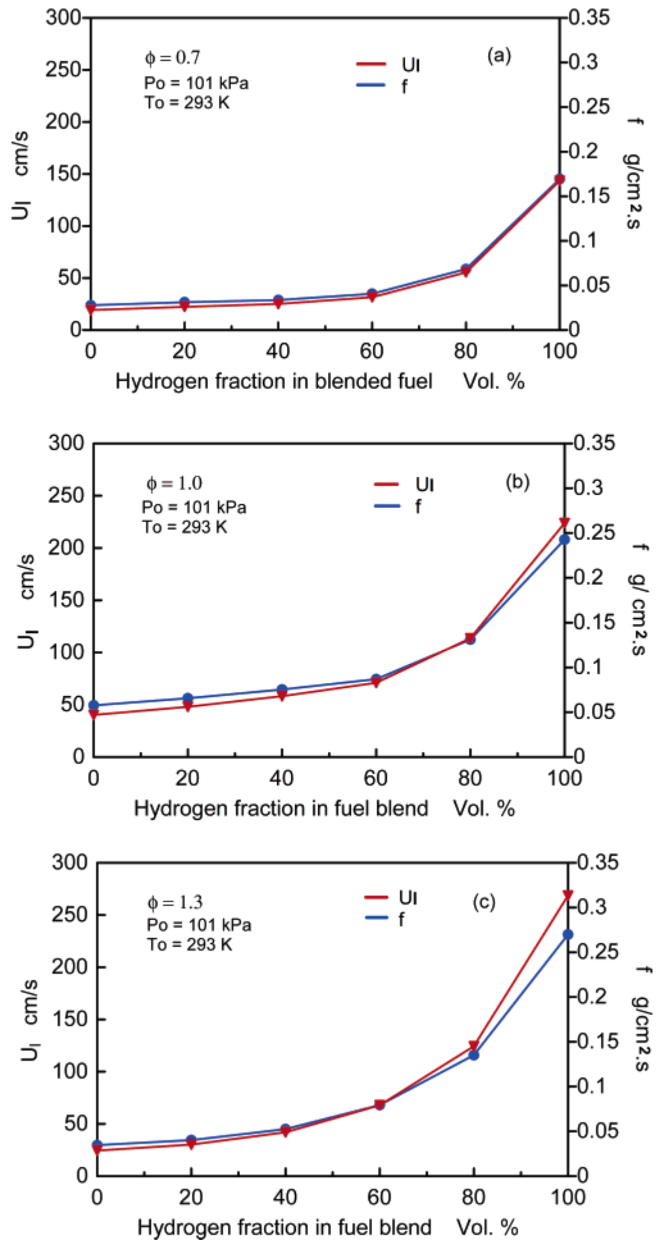

Figure 2. Unstretched laminar burning velocities and mass burning fluxes vs hydrogen fractions.

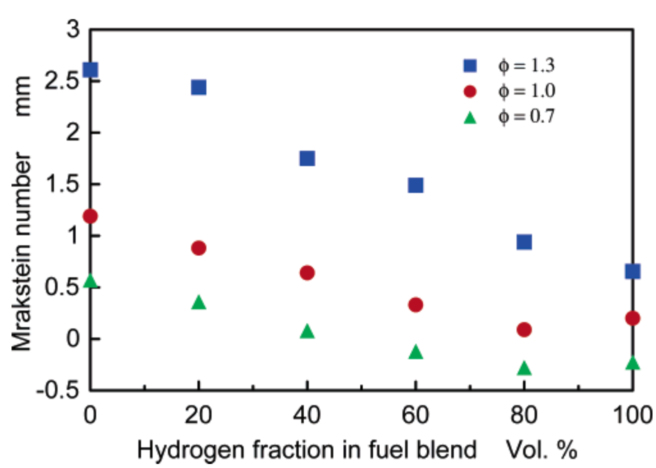

Figure 3. Markstein number vs hydrogen fraction at various equivalence ratios.

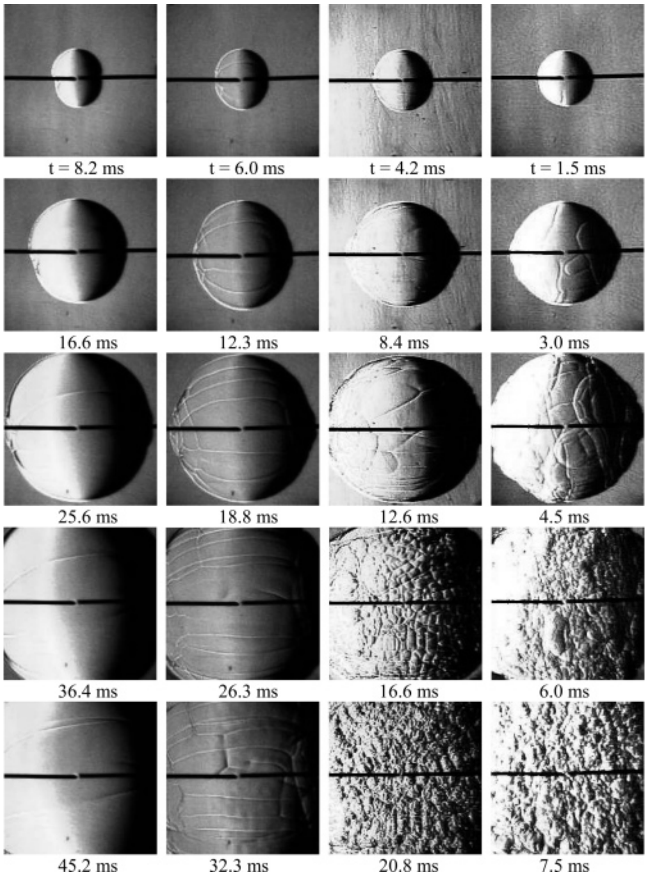

Figure 4. Schlieren photos of flame propagation at various hydrogen fractions and $\phi = 0.7$.

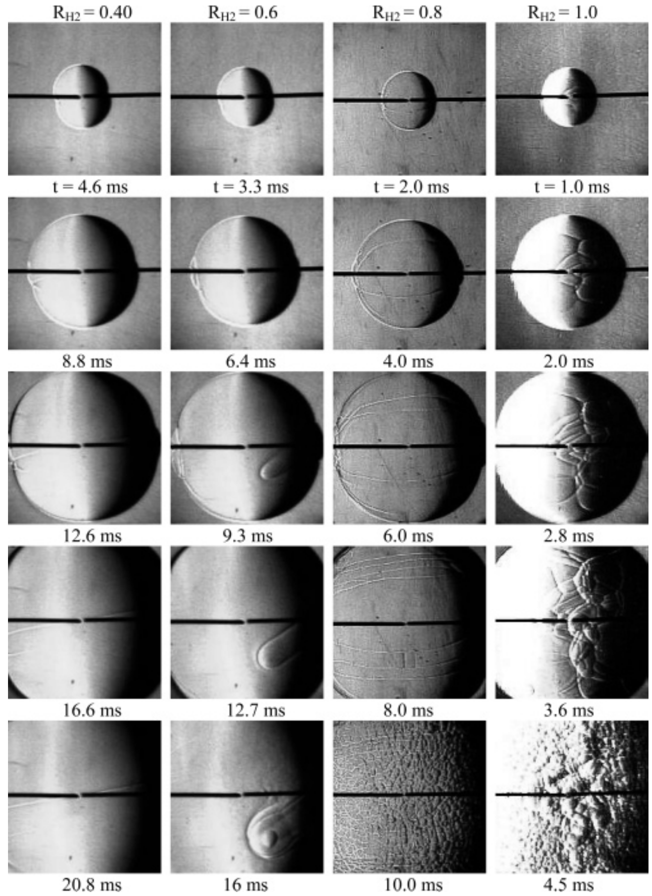

Figure 5. Schlieren photos of flame propagation at various hydrogen fractions and $\phi = 1.0$.

Figure 4 shows the flame photos at an equivalence ratio of 0.7 and hydrogen fractions R_{H_2} of 30%, 60%, 80%, and 100%. At the initial stage of flame propagation, the flame front keeps a smooth surface for all hydrogen fractions. In the case of 30% hydrogen fraction, a smooth front surface is maintained through the whole flame propagation process. In the case of 60% hydrogen fraction, small flaw and protruding occur at the flame front surface, and they will develop with the development of the flame. In the case of 80% and 100% hydrogen fractions, large flaw and protruding occur at a late stage of flame propagation, forming a cellular surface structure. This reveals that flame stability decreases with the increase of hydrogen fraction. Pure hydrogen combustion brings the highest flame instability, and flame front surface flaws will appear at the early stage of flame propagation, indicating the large thermodiffusive influence for lean hydrogen combustion.[12]

Figure 5 illustrates flame photos at an equivalence ratio of 1.0 and hydrogen fractions of 40%, 60%, 80%, and 100%. Similar to the case at lean mixture combustion ($\phi = 0.7$), the flame instability will increase with the increase of hydrogen fraction. However, large flaw and honeycomb-like surface appear at high hydrogen fraction (equal to or larger than 80%) and large flame radius. For hydrogen fraction of 40% and 60%, a smooth flame front surface can be sustained in the development of flame, and only at late stage will small numbers of surface flaws appear.

Figure 6 shows the flame photos of 60%, 80%, and 100% hydrogen fractions at an equivalence ratio of 1.3. The flame photo shows that good flame stability remains at various hydrogen fractions, even at large hydrogen fraction or pure hydrogen combustion. A smooth flame front surface is maintained at 60% and 80% hydrogen fractions, only for pure hydrogen combustion and at late stage of flame propagation does a flaw appear at the flame surface. For rich mixture combustion, the Markstein lengths always keep a positive value during flame propagation as shown in Figure 3; thus, flame stability can be sustained for rich mixture combustion. It can be concluded that flame stability will increase with the increase of equivalence ratio, and lean mixture combustion is easily leading to the flame instability while rich mixture combustion can maintain the flame stability.

Figure 7 gives the flame photos for various equivalence ratios and 80% hydrogen fraction. Flame photos show that the stability of flame increases with the increase of equivalence ratio. In the case of lean mixture combustion ($\phi = 0.7$), the flaw and protruding at flame front surface occur at early stage of flame development and honeycomb-like surface appears at late stage of flame development. In the case of stoichiometric mixture combustion ($\phi = 1.0$), the flaw and protruding at flame front surface occur at late stage of flame development. In the case of rich mixture combustion ($\phi = 1.3$), the flaw and protruding do not appear during flame propagation. This is consistent with the behavior of Markstein length versus equivalence ratio. That is, a large value of Markstein length corresponds to good flame stability whereas a small value of Markstein length reduces flame stability, a negative value of Markstein length gives high instability of flame. The study in other aspects provides the rationale for flame stability analysis from evaluation of Markstein length.

Instability of flame at early stage of flame development is mainly influenced by thermodiffusive factor. However, with flame development and flame radius increasing, hydrodynamic factor becomes the dominant factor.[12] For free diffusive flame,

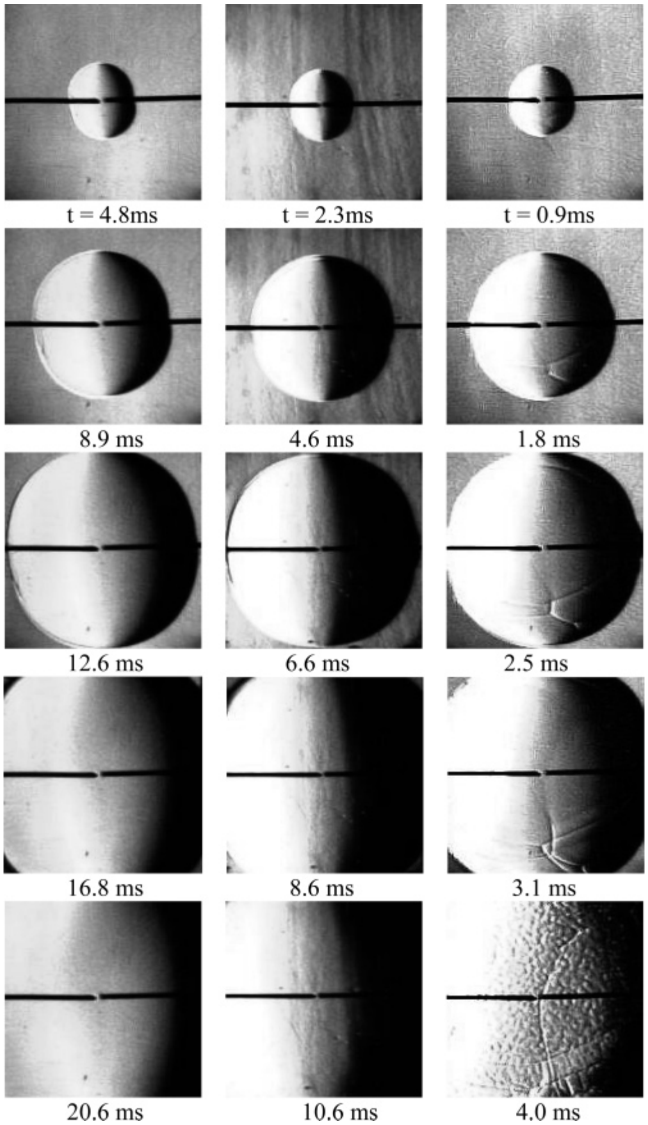

Figure 6. Schlieren photos of flame propagation at various hydrogen fractions and $\phi = 1.3$.

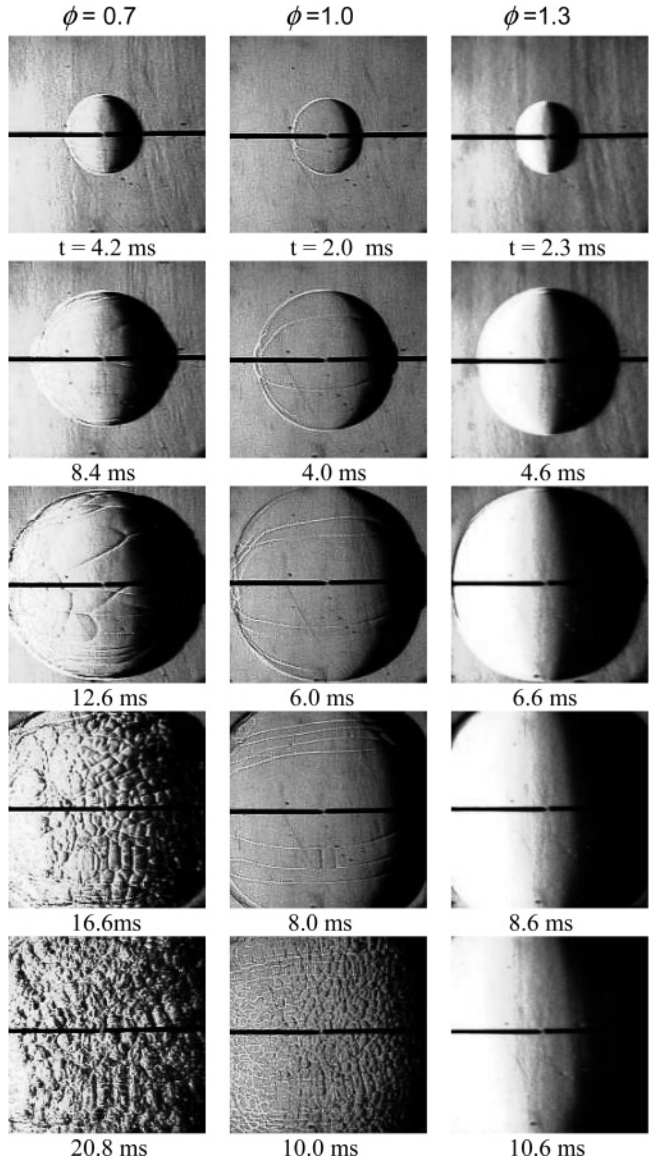

Figure 7. Schlieren photos of flame propagation at various equivalence ratios and 80% hydrogen fraction.

the instability of hydrodynamic is originated from gas thermal expansion,[6] where the ratio of unburned gas to burned gas at two sides of the flame front (ρ_u/ρ_b) and flame thickness (δ_l) can be qualitatively estimate the flame stability.[12] A high value of ρ_u/ρ_b tends to increase the flame instability while a large thickness of flame tends to decrease the flame instability. Figure 8 gives the value of ρ_u/ρ_b and the flame thickness versus hydrogen fractions at various equivalence ratios. ρ_u/ρ_b is determined from thermal equilibrium, and flame thickness δ_l is calculated from the ratio of viscosity of unburned gas ν to unstretched laminar burning velocity U_l, that is, $\delta_l = \nu/U_l$. The results show that, when the hydrogen fraction is less than 80%, ρ_u/ρ_b and flame thickness will decrease with the increase of hydrogen fraction, a decrease in ρ_u/ρ_b will decrease flame instability while a decrease in flame thickness will increase flame instability. Thus, flame stability is determined by combining the influence of the two factors. When the hydrogen fraction is larger than 80%, ρ_u/ρ_b is increased and flame thickness is decreased with the increase of hydrogen fraction. These two factors all lead to the increase of flame instability and easily form a hydrodynamically generated cellular surface at the flame front area.

Conclusions

Flame propagation characteristics of natural gas-hydrogen-air mixtures were studied in a constant volume combustion bomb at normal temperature and pressure. The main conclusions are summarized as follows:

(i) Unstretched laminar burning velocity and mass burning flux increase with the increase of hydrogen fraction in natural gas−hydrogen blend. Flame stability increases with the increase of equivalence ratio.

(ii) For a specific equivalence ratio, the Markstein length decreases with the increase of hydrogen fraction, leading to the increase of thermodiffusively generated flame instability. Flaws and protruding or even honeycomb-like structures occur at the flame front surface at lean mixture combustion while rich mixture combustion maintains a smooth flame front surface. Lean mixture increases the flame instability while rich mixture increases the flame stability.

(iii) At large flame radius, the hydrodynamic factor becomes the dominant influencing factor for flame instability. The ratio of unburned gas to burned gas at two side of flame front and the flame thickness can reflect the flame instability.

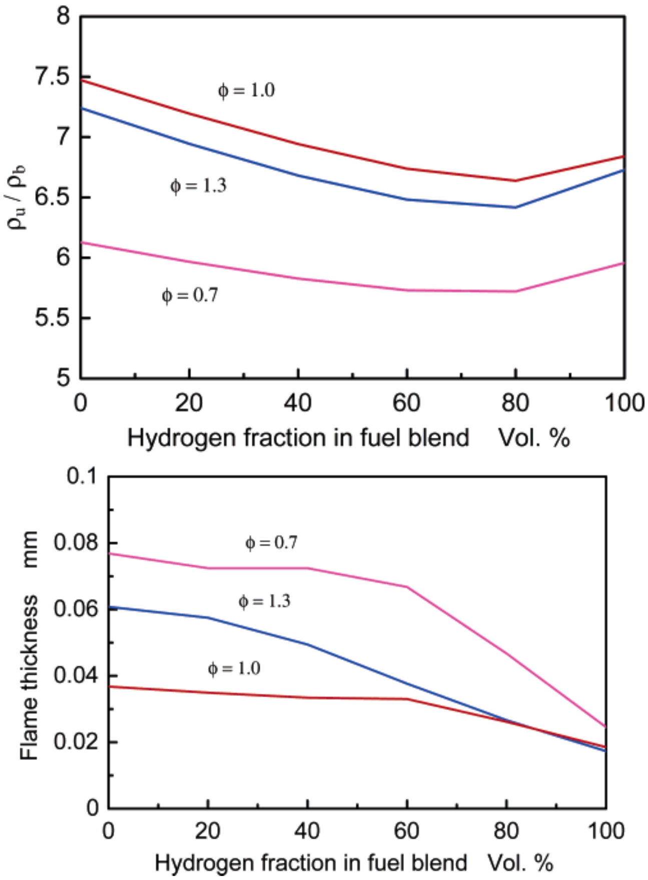

Figure 8. Density ratios and flame thicknesses vs hydrogen fractions at various equivalence ratios.

(iv) At large hydrogen fraction (larger than 80%), ρ_u/ρ_b is increased and the flame thickness is decreased with the increase of hydrogen fraction, leading to the increase of flame instability and easily forming the hydrodynamically generated cellular surface at flame front.

Acknowledgment. This study was supported by National Natural Science Foundation of China (50422261), National Basic Research Project (2003CB214501), and State Key Laboratory Award Fund from Natural Science Foundation of China (50323001). The authors acknowledge the students of Xi'an Jiaotong University for their help with the experiment and preparation of the manuscript. The authors also express their thanks to the colleagues of Xi'an Jiaotong University for their helpful comments and advice during the manuscript preparation.

Nomenclature

A = flame area

f = mass burning flux

L = molar number of air

L_b = Markstein number of burned gases

p_o = initial mixture pressure

r_u = flame radius

R_{H_2} = H_2(vol %)/[NG(vol %) + H_2(vol %)]; hydrogen volumetric fraction in fuel blend

S_l = unstretched flame speed

S_n = stretched flame speed

t = time

T_0 = mixture initial temperature

U_l = unstretched laminar burning velocity

ρ_b = density of burned gases

ρ_u = density of unburned gases

α = flame stretch rate

ϕ = equivalence ratio

δ_l = flame thickness (mm)

ν = viscosity of unburned gas

Subscripts

b = burned gases

u = unburned gases

EF060334V